ANL-6570

ANL-6570

Argonne National Laboratory

k CALCULATIONS FOR 22 ZPR-III FAST REACTOR ASSEMBLIES USING ANL CROSS-SECTION SET 635

by

W. G. Davey

LEGAL NOTICE

ANL-6570
Reactor Technology
(TID-4500, 17th Ed.)
AEC Research and
Development Report

ARGONNE NATIONAL LABORATORY
9700 South Cass Avenue
Argonne, Illinois

k CALCULATIONS FOR 22 ZPR-III FAST REACTOR ASSEMBLIES USING ANL CROSS-SECTION SET 635

by

W. G. Davey*

Idaho Division

*Assigned to Argonne National Laboratory from the United Kingdom Atomic Energy Authority

May 1962

Operated by The University of Chicago
under
Contract W-31-109-eng-38

TABLE OF CONTENTS

LIST OF FIGURES

LIST OF TABLES

k CALCULATIONS FOR 22 ZPR-III FAST REACTOR ASSEMBLIES USING ANL CROSS-SECTION SET 635

by

W. G. Davey

ABSTRACT

The Yiftah, Okrent, and Moldauer cross-section set (ANL Set 135) has been modified to include new measurements of ν and α for U^{235}, and also to include, in an approximate manner, Hummel, Rago, and Meneghetti's corrections for flux depression at resonance energies in aluminum and stainless steel. This modified set, ANL Set 635, has been used to compute values of k for 22 ZPR-III assemblies of widely varying composition. The DSN neutron transport code was used in spherical geometry and the S4 approximation; shape factors were used to convert from cylindrical to spherical geometry. Seventeen of the calculated values of k lie within $\pm 1\%$ of a mean value of 1.003, and the remaining 5 lie within $\pm 2\%$. In terms of prediction of critical mass, it appears that the procedure used here can achieve an accuracy of 5% to 10% for a wide range of U^{235}-fueled assemblies.

1. INTRODUCTION

The main objectives of Yiftah, Okrent, and Moldauer in constructing their published(1) multigroup cross-section set (ANL Set 135, widely known as the YOM Set) was to use, as far as was possible, only microscopic nuclear data, and to document all choices and assumptions made. In a comparison(1) between measured and calculated critical masses of a range of ZPR-III assemblies for which data were available at the time of the study, it was shown that the disagreement in terms of k_{eff} was, in general, only about 1% and was at most about 2%. In addition, it was shown that the use of conservative values for ν for U^{235} (which were not the best which could be deduced from the basic data but which were plausible in view of experimental errors) further reduced the disagreement between calculation and experiment.

Unfortunately, this fairly satisfactory situation did not continue when the range of ZPR-III experiments was extended to large reactors containing considerable quantities of nonfertile diluents, such as steel, aluminum,

carbon, and oxygen.[2-4] In these cases, the calculated values of k (not using the conservative values of ν for U^{235}) were about 5% too high. Recent work by Meneghetti[5,13] and Hummel and Rago[6] has shown that for materials such as aluminum, steel, sodium, and oxygen, which have strong resonances in the energy region of interest, group cross sections must be obtained in a manner that accounts for the depression of the flux in the resonances. Allowance for these effects has reduced the disagreement between calculation and experiment,[5,13] but if only this correction is introduced the discrepancies in certain cases still remain as high as 3% or 4% in k.

However, there are other points for which recent work has indicated that the original YOM calculations can be improved. In the field of analysis, calculations by Loewenstein and Main,[7] and experiments[20,21] have shown that the shape factors which should be used in deriving the masses of equivalent spherical reactors from those of the experimental cylindrical reactors (which is necessary as multigroup transport theory calculations are only practicable in one-dimensional geometry) in some cases are appreciably different from those previously used.[8] Also, new measurements show that the capture-to-fission ratios (α) for U^{233}, U^{235}, and Pu^{239}[9] and the ν value for U^{235}[10-12] are considerably different from the YOM data.

As each of the modifications (i.e., in resonance shielding effects, shape factors, and α and ν values) can change the calculated values of k in certain assemblies by up to 1%, it was believed that these should be introduced into a further study of the ZPR-III data.

For this study, the YOM data were modified to give a cross-section set listed at Argonne as ANL Set 635, and this was used to examine 22 ZPR-III assemblies of widely varying composition.

2. OBJECTIVE OF THIS STUDY

The work of Hummel and Rago and Meneghetti clearly shows that when reactors contain materials with strong resonances, then, due to the superposition of resonances, an exact evaluation of group cross sections must be made for the mixture of elements. Consequently, as all practical reactors contain steel and sodium, exact calculations must use cross-section sets which are unique to each core composition. In addition, as there are spatial variations of neutron spectrum, it is possible that in exact calculations group cross sections should vary throughout the reactor.

carbon, and oxygen.[2-4] In these cases, the calculated values of k (not using the conservative values of ν for U^{235}) were about 5% too high. Recent work by Meneghetti[5,13] and Hummel and Rago[6] has shown that for materials such as aluminum, steel, sodium, and oxygen, which have strong resonances in the energy region of interest, group cross sections must be obtained in a manner that accounts for the depression of the flux in the resonances. Allowance for these effects has reduced the disagreement between calculation and experiment,[5,13] but if only this correction is introduced the discrepancies in certain cases still remain as high as 3% or 4% in k.

However, there are other points for which recent work has indicated that the original YOM calculations can be improved. In the field of analysis, calculations by Loewenstein and Main,[7] and experiments[20,21] have shown that the shape factors which should be used in deriving the masses of equivalent spherical reactors from those of the experimental cylindrical reactors (which is necessary as multigroup transport theory calculations are only practicable in one-dimensional geometry) in some cases are appreciably different from those previously used.[8] Also, new measurements show that the capture-to-fission ratios (α) for U^{233}, U^{235} and Pu^{239}[9] and the ν value for U^{235}[10-12] are considerably different from the YOM data.

As each of the modifications (i.e., in resonance shielding effects, shape factors, and α and ν values) can change the calculated values of k in certain assemblies by up to 1%, it was believed that these should be introduced into a further study of the ZPR-III data.

For this study, the YOM data were modified to give a cross-section set listed at Argonne as ANL Set 635, and this was used to examine 22 ZPR-III assemblies of widely varying composition.

2. OBJECTIVE OF THIS STUDY

The work of Hummel and Rago and Meneghetti clearly shows that when reactors contain materials with strong resonances, then, due to the superposition of resonances, an exact evaluation of group cross sections must be made for the mixture of elements. Consequently, as all practical reactors contain steel and sodium, exact calculations must use cross-section sets which are unique to each core composition. In addition, as there are spatial variations of neutron spectrum, it is possible that in exact calculations group cross sections should vary throughout the reactor.

Although the amount of work involved in this procedure is, no doubt, justified for examination of a specific reactor design, a large amount of computation is concerned with parametric studies of projected reactors. In these studies, a large number of reactors of different compositions and sizes must be examined briefly in order to find which reactors are worthy of detailed study, and the work involved in exact calculations for these reactors could be prohibitive. Although such a procedure is known to be inexact, there is a strong case for determining if a single cross-section set can predict the critical sizes of a variety of reactors with adequate accuracy.

Hence, the objective of the present work is to see if a single cross-section set, based upon the basic nuclear data, can predict the critical masses of a wide variety of ZPR-III assemblies with reasonable accuracy.

It is recognized that, even if such a cross-section set is successful in attaining this objective, there is no expectation that it can predict other parameters with similar accuracy, and, indeed, it may be grossly in error in computation of, for example, perturbation effects.

3. CONSTRUCTION OF ANL SET 635

The ANL cross-section set 635 consists of the 16-group YOM Set (ANL Set 135) with modified values of α and ν for U^{235} and of σ transport (σ_{tr}) and σ elastic removal (σ_{er}) for aluminum and the components of stainless steel, i.e. Fe, Ni, and Cr.

3.1 α for U^{235}

This quantity has been measured by Diven and Hopkins[9] over an energy range from 30 kev to 1 Mev with about ±7% accuracy.

Values of α for each of the YOM groups in the range of the measurements were taken from a smooth curve drawn through the experimental points of Diven and Hopkins. These were then used with the YOM values of σ_f for U^{235} to give new $\sigma(n,\gamma)$ U^{235} data. For YOM groups 1, 2, 3, 15, and 16, the YOM $\sigma(n,\gamma)$ U^{235} were used. The two sets of data are compared in Table I.

It can be seen that the new values of $\sigma(n,\gamma)$ are lower than those provided by the YOM data above about 0.3 Mev (i.e., groups 4, 5, 6) and higher than those from the YOM data below this energy. As many of the ZPR-III assemblies are not very dilute, they have spectra which peak at about this energy, and in these cases (e.g., assemblies 23, 10, and 24) the change in k caused by the change in $\sigma(n,\gamma)$ U^{235} is small (0.2% or less), but in very dilute assemblies (e.g., assemblies 14 and 29) the value of k is decreased by about 1%.

Table I

ANL SET 635 AND YOM DATA FOR $\sigma(n,\gamma)$ AND ν U^{235}

Group (j)	Lower Energy Limit (E_L) (Mev)	$\sigma(n,\gamma)$ (barns)		ν	
		Set 635	YOM	Set 635[a]	YOM
1	3.668	0.020	0.020	2.71	3.15
2	2.225	0.035	0.035	2.71	2.84
3	1.350	0.058	0.058	2.60	2.67
4	0.825	0.102	0.115	2.53	2.58
5	0.500	0.167	0.193	2.48	2.52
6	0.300	0.200	0.240	2.46	2.48
7	0.180	0.305	0.296	2.44	2.45
8	0.110	0.397	0.370	2.43	2.44
9	0.067	0.549	0.483	2.43	2.43
10	0.0407	0.731	0.624	2.42	2.43
11	0.0250	0.954	0.803	2.42	2.42
12	0.0150	1.150	1.003	2.42	2.42
13	0.0091	1.396	1.249	2.42	2.42
14	0.0055	1.732	1.689	2.42	2.42
15	0.0021	2.092	2.092	2.42	2.42
16	0.0005	3.825	3.825	2.42	2.42

[a]These are the conservative ν values of YOM

3.2 ν for U^{235}

The data for ν of U^{235} as a function of neutron energy has been greatly extended and improved in accuracy by the work of Moat et al., Butler et al., and Diven and Hopkins, and it is apparent that these data should be carefully analyzed to obtain the maximum information. For example, it is now clear that ν of U^{235} is not a linear function of neutron energy from thermal energies to 14 Mev,(10) and it is possible that it may not be linear in the energy range of interest in fast reactors. However, this point is not yet clear, and the new data are not inconsistent with the conservative values tabulated by YOM (these are given approximately as $\nu(E) = 2.42 + 0.1E$). Consequently, in order to avoid unnecessary duplication of data, it was decided to use the conservative YOM values in the present study. These data are given in Table I.

A feature of these values that probably will not be substantiated by the new measurements is the equality of ν in groups 1 and 2. However, as only about 2 to 3% of the flux lies in group 1, and also as the final analysis of the experimental data will certainly require some modification of all the ν values, it was decided to accept these data.

As has been shown by Yiftah, Okrent, and Moldauer,[1] use of the conservative ν values rather than of the best YOM data decreases the calculated values of k by about $1\frac{1}{2}$%.

3.3 Resonance-corrected Cross Sections for Aluminum and Stainless Steel

The IBM-704 ELMOE code of Hummel and Rago carries out a fundamental mode analysis by means of hundreds of neutron groups and detailed elastic-scattering matrices, so that resonances are accurately described. The code thus yields the material buckling of the core under consideration and the detailed variation of flux with energy. Gross group cross-sections for neutron transport and elastic scattering are then derived.

As stated in Section 2, the ELMOE calculation should be carried out for the correct core mixture and a given mixture which contains resonance materials, such as aluminum, stainless steel, sodium, and oxygen, should have a unique set of cross sections, but the present study is concerned with determining the usefulness of a single cross-section set. Here we follow the work of Meneghetti in that we use aluminum and stainless steel cross sections evaluated, respectively, for the predominantly aluminum and stainless-steel-diluted ZPR-III Assemblies 23 and 32. Hummel and Rago and Meneghetti showed that this procedure overestimates the correction applied for resonance flux depression, since the minima in the cross section of a given element are frequently filled in by other elements. The reader is referred to these reports for discussions of this phenomenon.

Thus, in neither the aluminum nor the stainless steel data in Set 635 is allowance made for the presence of other resonance materials. The cross sections for sodium, oxygen, and all other materials (excluding U^{235}) were taken unmodified from the YOM set.

The corrections to the YOM aluminum and stainless steel data are taken from Table II of Meneghetti.[13] They are presented in Table II of this report. These correction factors were applied to the YOM data for Al, Fe, Ni, and Cr to give the cross sections used in Set 635. As, in each group, the same stainless steel correction factor was applied to the Fe, Ni, and Cr YOM cross sections, these data can only be used for calculating the effects of stainless steel. They cannot be used for evaluating the effects of Fe, Ni, and Cr separately.

Meneghetti has shown that for ZPR-III Assemblies 23, 29, 30, 31, and 32, the effect of introducing the corrections listed in Table II is to reduce the calculated value of k.

Table II

RATIO OF MODIFIED (SET 635) TO UNMODIFIED (YOM) CROSS SECTIONS FOR ALUMINUM AND STAINLESS STEEL

Group (j)	Lower Energy Limit E_L (Mev)	Ratio			
		Aluminum		Stainless Steel	
		Transport	Elastic Transfer	Transport	Elastic Transfer
1	3.668	(1)[a]	(1)	(1)	(1)
2	2.225	0.83	1.11	0.86	0.81
3	1.350	0.95	1.25	0.97	1.14
4	0.825	0.85	1.02	0.91	1.03
5	0.500	0.945	1.11	0.95	1.11
6	0.300	0.94	1.02	0.86	0.78
7	0.180	0.76	0.93	0.94	1.03
8	0.110	0.61	0.84	0.84	0.99
9	0.067	0.475	0.61	0.64	0.80
10	0.0407	0.67	0.68	0.95	0.95
11	0.0250	0.24	0.36	0.49	0.75
12	0.0150	0.71	~0	0.67	0.73
13	0.0091	0.97	1.00	0.98	0.98
14	0.0055	(1)	(1)	(1)	(1)
15	0.0021	(1)	(1)	(1)	(1)
16	0.0005	(1)	(1)	(1)	(1)

[a]For groups 1, 14, 15, and 16, no ELMOE calculation was made and here the ratio is assumed to be unity.

4. CALCULATIONS WITH SET 635

The method used in the present calculations was (a) to correct the experimental critical mass for the effects of heterogeneity, core boundary irregularities, and the ZPR-III center gap to give the critical mass of a homogeneous regular system, usually a cylinder; (b) except in the few cases where the experimental cores were spherical, a shape factor was next applied to give the critical mass of an equivalent homogeneous spherical reactor; (c) and to carry out spherical geometry, DSN transport theory calculations in the S4 approximation to obtain the effective multiplication factor k. Ideally, a k of unity should be obtained. From these calculations, spectra and fission rates can be derived.

The experimental critical masses and corrections are given in Table III.

Table III

EXPERIMENTAL CRITICAL MASSES AND CORRECTIONS[a]

ZPR-III Assembly Number	Experimental Critical Mass M (kg)	$\frac{(\Delta M/M)^b}{(\Delta k/k)}$	Experimental Corrections to Critical Mass			
			Hetero-geneity (kg)	Irregular Boundary (kg)	Center Gap (kg)	Corrected Experimental Mass (kg)
2A	147.7	3.3	+ 3.8	-0.1	-1.1	150.3
5	159.5	4.1	+ 4.6	-0.1	-1.2	162.8
6F	131.1	3.8	+ 3.4	-0.1	-1.1	133.3
9A	146.2	4.4	+ 5.8	-0.1	-1.3	150.6
10	155.8	5.3	+ 9.1	-0.1	-1.7	163.1
11	240.6	7.0	+16.6	-0.2	-3.0	254.0
12	176.8	5.5	+ 5.8	-0.1	-1.8	180.7
14	136.0	3.8	+ 2.6	-0.1	-1.1	137.4
16	204.8	4.8	+10.2	-0.2	-2.0	212.8
17	156.5	4.5	+ 3.5	-0.1	-1.4	158.5
20	431.0	5.0	+15.2	-0.2	-3.0	443.0
23	258.1	4.5	+ 9.8	-0.2	-3.0	264.7
24	460.7	9.4	+35.7	-0.4	-6.0	490.0
25	581.6	7.2	+37.7	-0.4	-6.0	612.9
29	420.7	5.4	+24.0	-0.2	-3.0	441.5
30	394.9	5.7	+22.5	-0.2	-3.0	414.2
31	463.0	5.6	+25.9	-0.2	-3.0	485.7
32	227.5	4.2	+ 9.7	-0.2	-3.0	234.0
33	238.0	4.2	+ 9.7	-0.2	-3.0	244.5
34	503.0	5.0	+24.9	-0.4	-6.0	221.5
35	505.4	4.8	+33.5	-0.4	-6.0	532.5
36	242.7	4.3	+10.4	-0.2	-3.0	249.9

[a]References for these data are given in Appendix I

[b]This ratio is that between a fractional change in critical mass (added at the boundary of the reactor with no change in composition) and the corresponding fractional change in k.

4.1 Corrections for Heterogeneity, Core-boundary Irregularities, and the ZPR-III Central Gap

The basic units for construction of the ZPR-III assemblies are small slabs of fuel and diluent of approximate dimensions $2 \times 2 \times \frac{1}{4}$ in. It has been shown both experimentally(14) and theoretically(15) that, because of the finite thickness of the pieces, the fission rates are not uniform through a typical cell, but are higher in the fuel. As a consequence, the experimental heterogeneous assembly is more reactive than a similar homogeneous system. Experimental corrections for this effect are made by measuring the reactivity change on bunching the fuel pieces and also on substituting some $\frac{1}{16}$-in.-thick fuel pieces and then extrapolating to find the effect of zero-thickness fuel. These reactivity effects are of the order of 1% in k (i.e., 5% to 10% in critical mass).

The correction for core-boundary irregularities arises because cylindrical and spherical assemblies must be approximated in ZPR-III by means of modules of square cross section. Experiments(14) in which smaller modules were utilized have indicated that the correction is small; the experimental assembly is less reactive than the ideal system by only about 0.01% to 0.02% in k (i.e., about 0.1% in critical mass).

The center-gap correction in ZPR-III occurs because it is constructed in two halves and there is an inhomogeneity in the center plane, consisting of the fronts of the drawers used to hold the fuel and diluent pieces (about 0.16 cm of stainless steel or aluminum) plus any clearance between the halves. It has been estimated that these cause the experimental assembly to be less reactive than the ideal system by about 0.1% to 0.2% in k (i.e., about 1% in critical mass).

It can be seen that by far the most important of these corrections is that made for heterogeneity. Because of uncertainties in extrapolation to zero fuel thickness and in the validity of the substitutions, it is possible that this correction may be uncertain to about 0.2% to 0.3% in k. Errors in the other corrections are probably small when compared with this error.

Because of the lack of experimental data for some reactors, it was necessary to estimate the magnitude of some corrections by considering the results obtained with similar reactors.

4.2 Shape-factor Corrections

The shape factor (SF) is defined as the ratio of the spherical critical mass of a system to that of an assembly of the same core and blanket composition but of different geometry (usually cylindrical).

It has long been known that the SF is a function of the length-to-diameter ratio (L/D) of a cylindrical core, and it appears reasonable that it should also be dependent upon other reactor parameters such as core size and core and blanket composition. Until recently, the only data available were experimental values for small dense cores [e.g., see Loewenstein and Okrent.](16) Although a recent theoretical study by Loewenstein and Main(7) and some ZPR-III measurements(20,21) have extended our knowledge to some large dilute cores, it still does not seem possible to select a SF unambiguously.

The author understands that some of the numerical data given by Loewenstein and Main(7) may be subject to revision; hence, the procedure adopted here was to use Loewenstein and Main's data to define the variation of SF with L/D and to obtain absolute values using experimental data only.

The correction for core boundary irregularities arises because cylindrical and spherical assemblies must be approximated in ZPR-III by means of modules of square cross section. Experiments[14] in which smaller modules were utilized have indicated that the correction is small; the experimental assembly is less reactive than the ideal system by only about 0.01% to 0.02% in k (i.e., about 0.1% in critical mass).

The center-gap correction in ZPR-III occurs because it is constructed in two halves and there is an inhomogeneity in the center plane consisting of the fronts of the drawers used to hold the fuel and diluent pieces (about 0.16 cm of stainless steel or aluminum) plus any clearance between the halves. It has been estimated that these cause the experimental assembly to be less reactive than the ideal system by about 0.1% to 0.2% in k (i.e., about 1% in critical mass).

It can be seen that by far the most important of these corrections is that made for heterogeneity. Because of uncertainties in extrapolation to zero fuel thickness and in the validity of the substitutions, it is possible that this correction may be uncertain to about 0.2% to 0.3% in k. Errors in the other corrections are probably small when compared with this error.

Because of the lack of experimental data for some reactors, it was necessary to estimate the magnitude of some corrections by considering the results obtained with similar reactors.

4.2 Shape-factor Corrections

The shape factor (SF) is defined as the ratio of the spherical critical mass of a system to that of an assembly of the same core and blanket composition but of different geometry (usually cylindrical).

It has long been known that the SF is a function of the length-to-diameter ratio (L/D) of a cylindrical core, and it appears reasonable that it should also be dependent upon other reactor parameters such as core size and core and blanket compositions. Until recently, the only data available were experimental values for small dense cores (e.g., see Loewenstein and Okrent[16]). Although a recent theoretical study by Loewenstein and Main[7] and some ZPR-III measurements[20,21] have extended our knowledge to some large dilute cores, it still does not seem possible to select a SF unambiguously.

The author understands that some of the numerical data given by Loewenstein and Main[7] may be subject to revision; hence, the procedure adopted here was to use Loewenstein and Main's data to define the variation of SF with L/D and to obtain absolute values using experimental data only.

Loewenstein and Main show that the general variation of SF with L/D is similar for the four cases investigated, all the curves giving a maximum SF close to an L/D of 0.9. Accordingly, a mean curve giving this variation was derived from the data of Loewenstein and Main, the curve being normalized to a value of unity at L/D = 0.9.

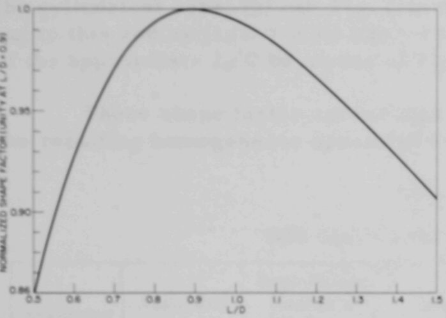

Fig. 1. Normalized Shape Factor as a Function of L/D

The shape of this mean curve (see Fig. 1) is within about $\frac{1}{2}$% of the exact Loewenstein and Main values over the L/D range from 0.7 to 1.2.

Most of the experimental data on shape factors has been summarized by Loewenstein and Main, with the only data given for U^{235}-fueled, thick uranium-reflected systems being for Topsy and the spherical ZPR-III Assemblies 6F and 9A. These data have now been extended for spherical versions of the large ZPR-III Assemblies 24 and 31 (called Assemblies 38 and 39, respectively). With the five values available, the only well-defined trend is of decrease of SF with increasing core size, the SF being roughly a linear function of core radius.

This variation is shown in Fig. 2, the shape factors being calculated for cylinders with L/D values of 0.9.

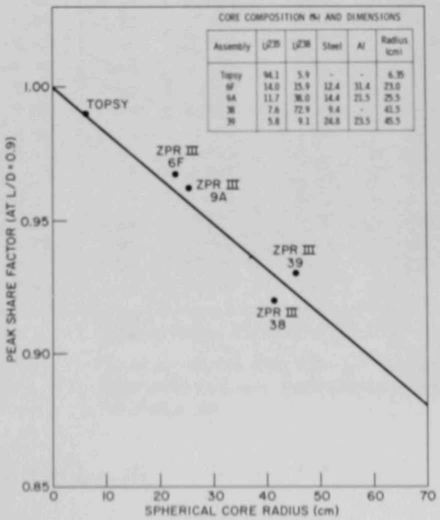

CORE COMPOSITION (%) AND DIMENSIONS

Assembly	U^{235}	U^{238}	Steel	Al	Radius (cm)
Topsy	94.1	5.9	-	-	6.35
6F	14.0	15.9	12.4	31.4	23.0
9A	11.7	38.0	14.4	21.5	25.5
38	7.6	72.9	9.4	-	41.5
39	5.8	9.1	24.8	23.5	45.5

Fig. 2

Peak Shape Factor Versus Core Radius

Loewenstein and Main show that the general variation of SF with L/D is similar for the four cases investigated, all the curves giving a maximum SF close to an L/D of 0.9. Accordingly, a mean curve giving this variation was derived from the data of Loewenstein and Main, the curve being normalized to a value of unity at L/D = 0.9.

Fig. 1. Normalized Shape Factor as a Function of L/D

The shape of this mean curve (see Fig. 1) is within about 2% of the exact Loewenstein and Main values over the L/D range from 0.7 to 1.2.

Most of the experimental data on shape factors has been summarized by Loewenstein and Main, with the only data given for U^{235}-fueled, thick uranium-reflected systems being for Topsy and the spherical ZPR-III Assemblies 6F and 9A. These data have now been extended for spherical versions of the large ZPR-III Assemblies 24 and 31 (called Assemblies 38 and 39, respectively). With the five values available, the only well-defined trend is of decrease of SF with increasing core size, the SF being roughly a linear function of core radius.

This variation is shown in Fig. 2, the shape factors being calculated for cylinders with L/D values of 0.9.

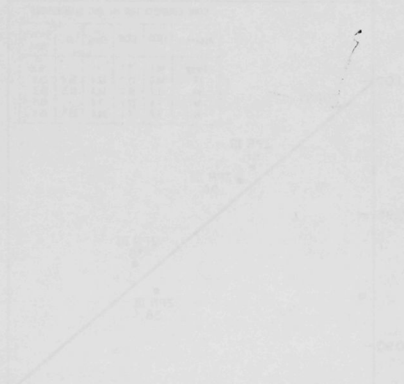

Fig. 2

Peak Shape Factor Versus Core Radius

Thus, as little data are available, the possible variation of shape factor with reactor composition, etc., has had to be ignored, and only a crude dependence upon core size can be introduced.

The procedure for obtaining shape factors to permit computations was therefore (a) to calculate the radius of a sphere of the same volume as the cylindrical core; (b) use Fig. 2 to find the peak shape factor corresponding to this radius (L/D = 0.9); and (c) to correct this shape factor to that of the appropriate L/D by means of Fig. 1.

These shape factor corrections are given in Table IV together with the resulting homogeneous spherical critical masses.

Table IV

THE SHAPE FACTOR CORRECTION

Radius

Assembly No.	Assembly Volume (liters)	Approximate Radius of Sphere of Same Volume (cm)	Peak Shape[a] Factor	L/D	f(L/D)[b]	Actual Assembly Shape Factor[c]	Critical Mass of Sphere[d] (kg)
2A	56.4	24	0.96	0.97	0.997	0.96	144
5	60.8	24	0.96	0.94	0.999	0.96	156
6F	49.9	23	0.96	Sphere	-	-	133
9A	66.6	25 *	0.96	Sphere	-	-	151
10	70.1	~~28~~ 25.63	0.95	1.04	0.990	0.94	153
11	134.9	32 31.8	0.94	0.88	1.000	0.94	239
12	100.5	29	0.95	0.87	1.000	0.95	172
14	77.3	26	0.96	0.99	0.996	0.96	132
16	116.4	30	0.95	0.91	1.000	0.95	202
17	89.0	28	0.95	0.93	1.000	0.95	151
20	377.4	45	0.92	0.96	0.998	0.92	408
23	148.5	33	0.94	0.84	0.998	0.94	249
35 spherical version 24	324.6	43 42.9	0.93	0.93	1.000	0.93	456
25	432.6	47 47.01	0.92	0.90	1.000	0.92	564
29	451.5	48	0.92	0.79	0.992	0.91	402
30	356.4	44	0.92	0.80	0.994	0.91	377
31	425.0	47	0.92	0.73	0.980	0.90	437
32	131.0	32 31.56	0.94	1.17	0.972	0.91	213
33	136.9	32	0.94	1.14	0.977	0.92	225
34	574.4	52	0.91	0.94	0.999	0.91	475
35	663.9	54	0.91	1.00	0.995	0.91	485
36	138.1	32	0.94	1.44	0.920	0.87	217

[a]At L/D = 0.90, from Fig. 2

[b]From Fig. 1

[c](Peak Shape Factor) x [f(L/D)]

[d]Product of the shape factor and the corrected experimental mass given in Table III

* Based on 18.07" long x 17.41" diameter. 28 seems to be wrong

4.3 The DSN Calculations

The homogeneous spherical critical masses given in Table IV were used together with the core compositions to compute the expected critical radii. DSN, S4 calculations were then carried out to obtain k effective for each system. In all cases 30-mesh intervals were used, 15 being evenly spaced in the core and 15 in the reflector. In five cases, the calculations were repeated with double the number of mesh points, but this produced less than 0.03% change in k, and it was concluded that 30-mesh intervals described the system adequately.

Details of the reactor compositions are given in Appendix II.

5. RESULTS OF THE CALCULATIONS

The k values obtained from the DSN calculations are given in Table V together with a summary of the reactor compositions.

More accurate Appendix 2.

Table V

REACTOR COMPOSITIONS AND COMPUTED VALUES OF k

Assembly No.	Ratio U^{238}/U^{235}	Approximate Volume Percentage of Material in Core[a]									Computed k_{eff}	Deviation from Mean k of 1.003[b]	Equivalent Deviation in Critical Mass (%)[c]
		U^{235}	U^{238}	Steel	Al	Na	C	O	Mo	Zr			
23	0.07	9.3	0.7	9.2	42.8						1.012	+0.009	+4.1
2A	0.07	14.0	1.0	27.8	31.4						1.012	+0.009	+3.0
6F	1.1	14.0	15.9	12.4	31.4						1.008	+0.005	+1.9
5	1.1	14.0	15.9	12.3	31.4						1.010	+0.007	+2.9
29	2.0	5.0	10.0	24.9	24.4			14.5			1.005	+0.002	+1.1
30	1.5	5.9	9.0	24.7	23.4			7.3			1.014	+0.011	+6.3
31	1.6	5.8	9.1	24.8	23.5						1.013	+0.010	+5.6
34	2.2	4.7	10.3	24.8	25.5		9.1				1.000	-0.003	-1.5
9A	3.2	11.7	38.0	14.4	21.5						1.003	0.000	0.0
20	3.1	6.1	19.0	14.5	25.1				5.0	4.3	0.997	-0.006	-3.0
10	4.9	11.9	57.9	19.5							1.000	-0.003	-1.6
11	7.5	9.5	71.7	9.2							0.995	-0.008	-5.6
24	9.6	7.6	72.9	9.4							0.996	-0.007	-6.6
25	10.3	7.2	74.2	9.2							0.991	-0.012	-8.6
35	0.07	4.1	0.3	50.0		35.6		4.2			0.985	-0.018	-8.6
36	5.3	9.4	49.5	12.8		18.2					0.995	-0.008	-3.4
33	0.07	9.3	0.7	64.2		18.2					1.017	+0.014	+5.9
32	0.07	9.3	0.7	81.8							1.018	+0.015	+6.3
16	5.3	9.4	50.1	9.2			18.1				1.000	-0.003	-1.4
12	3.8	9.4	35.4	9.2			32.0				0.998	-0.005	-2.8
17	2.2	9.4	20.6	9.2			45.7				0.998	-0.005	-2.3
14	0.07	9.4	0.7	9.2			63.9				0.995	-0.008	-3.0

[a] At densities corresponding to the atomic densities tabulated by YOM.(1) These are also used for ANL Set 635.

[b] The average value of the computed k is 1.003.

[c] Using the $(\Delta M/M)/(\Delta k/k)$ values of Table III.

For completeness, the central spectra and the central spectral indices (principally fission ratios) were calculated; these are given in Appendix III. The group fission cross sections used in calculating the

4.3 The DSN Calculations

The homogeneous spherical critical masses given in Table IV were used together with the core compositions to compute the expected critical radii. DSN, S4 calculations were then carried out to obtain k effective for each system. In all cases 30-mesh intervals were used, 15 being evenly spaced in the core and 15 in the reflector. In five cases, the calculations were repeated with double the number of mesh points, but this produced less than 0.01% change in k, and it was concluded that 30-mesh intervals described the system adequately.

Details of the reactor compositions are given in Appendix II.

5. RESULTS OF THE CALCULATIONS

The k values obtained from the DSN calculations are given in Table V together with a summary of the reactor compositions.

For completeness, the central spectra and the central spectral indices (principally fission ratios) were calculated; these are given in Appendix III. The group fission cross sections used in calculating the average cross sections for U^{234} and U^{236} are not given by YOM, and values for these were estimated from the Second Edition of BNL-325. These are given in Appendix IV.

6. DISCUSSION OF THE CALCULATED VALUES OF k AND CONCLUSIONS

Examination of Table V shows that Set 635 is quite successful in that 17 of the calculated k values lie within $\pm 1\%$ of a mean value of 1.003, and the remaining 5 lie within $\pm 2\%$. This accuracy corresponds to an ability to predict the critical masses of 14 of the assemblies to better than $\pm 5\%$, and the remaining 8 to better than $\pm 10\%$.

If the nuclear data for a particular nuclide were appreciably in error, then it might be expected that there would be a tendency towards an increasingly inaccurate calculated value of k as the fraction of that nuclide was increased. The k values in Table V are grouped in a manner which would show such trends, but, although there are apparently slight tendencies, such as (a) a lower k as the U^{238}/U^{235} ratio increases and (b) lower k than average for all the carbon-containing assemblies, it is doubtful if these trends are meaningful. The apparent absence of such trends does not necessarily mean that the nuclear data are correct as, for example, errors in the transport and capture cross sections of a nuclide could fortuitously cancel out in a k calculation. In addition, any trends would tend to be masked by random errors in the analysis.

In fact, the spread of calculated values of k is consistent with their being a statistical distribution, for the root-mean-square deviation from the mean value of 1.003 is 0.009, and 16 k values lie within ± 0.009 of the mean and the remaining 6 lie between 0.009 and 0.018.

Hence, to summarize, it appears that a single cross-section set is capable of predicting critical sizes with an accuracy of 5 to 10%. This result, although encouraging, should be treated with caution, and it is perfectly feasible that the procedures adopted here have inadvertently obscured errors and that these errors may be magnified in somewhat different systems.

ACKNOWLEDGEMENTS

The author wishes to thank F. W. Thalgott for his encouragement of this work and W. B. Loewenstein for valuable criticism of an early draft of this report.

REFERENCES

1. S. Yiftah, D. Okrent, and P. A. Moldauer, Fast Reactor Cross-sections, Pergamon Press, New York (1960).

2. A. L. Hess, W. Gemmell, J. K. Long, and R. L. McVean, Critical Studies of a 450-liter Uranium Oxide Fast Reactor Core (ZPR-III Assembly 29), ANL-6336 (May 1961).

3. P. I. Amundson, A. L. Hess, W. P. Keeney, J. K. Long, and R. L. McVean, Critical Studies of a Dilute Oxide Fast Reactor Core (ZPR-III Assembly 30), ANL-6337 (May 1961).

4. R. J. Huber, J. K. Long, R. L. McVean, and J. M. Gasidlo, Critical Studies of a Dilute Carbide Fast Reactor Core (ZPR-III Assembly 34), ANL-6401 (May 1961).

5. D. Meneghetti, Recent Advances and Problems in Theoretical Analyses of ZPR-III Fast Critical Assemblies, Paper presented at IAEA-sponsored Seminar on the Physics of Fast and Intermediate Reactors, Vienna (1961), Paper No. SM-18/37.

6. H. H. Hummel and A. L. Rago, An Accurate Treatment of Resonance Scattering in Light Elements in Fast Reactors, Paper presented at the IAEA-sponsored Conference on the Physics of Fast and Intermediate Reactors, Vienna (1961), Paper No. SM-18/45.

7. W. B. Loewenstein and G. W. Main, Fast Reactor Shape Factors and Shape-dependent Variables, ANL-6403 (November 1961).

8. Figure 6-2 of Reactor Physics Constants, ANL-5800 (1958).

9. B. C. Diven and J. C. Hopkins, Capture-to-fission Ratios for Fast Neutrons in U^{233}, U^{235}, and Pu^{239}, IAEA-sponsored Seminar on the Physics of Fast and Intermediate Reactors, Vienna (1961), Paper No. SM-18/55.

10. A. Moat, D. S. Mather, and P. Fieldhouse, The Number of Prompt Neutrons from U^{235} Fission over the Range 0.04 to 3.0 Mev, IAEA-sponsored Seminar on Physics of Fast and Intermediate Reactors, Vienna (1961), Paper No. SM-18/18.

11. D. Butler, S. Cox, J. Meadows, J. Roberts, A. Smith, and J. Whalen, Experimental Study of Fission Properties Utilized in Reactor Design, IAEA-sponsored Seminar on the Physics of Fast and Intermediate Reactors, Vienna (1961), Paper No. SM-18/36.

12. B. D. Diven and J. C. Hopkins, Numbers of Prompt Neutrons per Fission for U^{233}, U^{235}, Pu^{239} and Cf^{252}, IAEA-sponsored Seminar on the Physics of Fast and Intermediate Reactors, Vienna (1961), Paper No. SM-18/56.

13. D. Meneghetti, Effect of Resonance Scattering on Criticality Calculations of Fast Assemblies, ANL-6466 (December 1961).

14. J. K. Long et al., Fast Neutron Power Reactor Studies with ZPR-III, Proceedings of the Second United Nations International Conference on the Peaceful Uses of Atomic Energy, Geneva, Switzerland, 12, 119 (1958).

15. D. Meneghetti and M. F. Loomis, Calculation of Heterogeneity Effects in ZPR-III Fast Assemblies Using the DSN Program, ANL-6218 (November 1960).

16. W. Loewenstein and D. Okrent, The Physics of Fast Power Reactors, A Status Report, Proceedings of the Second United Nations International Conference on the Peaceful Uses of the Atomic Energy, Geneva, Switzerland, 12, 16 (1958).

17. J. K. Long, et al., Experimental Results on Large Dilute Fast Critical Systems with Metallic and Ceramic Fuels, Paper presented at the IAEA-sponsored Seminar on the Physics of Fast and Intermediate Reactors, Vienna (1961), Paper No. SM-18/48.

18. J. M. Gasidlo, J. K. Long, R. L. McVean, Critical Studies of a Dilute Fast Reactor Core (ZPR-III Assembly 31), ANL-6338 (October 1961).

19. J. M. Gasidlo, J. K. Long, R. L. McVean, Critical Studies of a Fast Reactor Core Containing Depleted Uranium and Sodium as Diluents (ZPR-III Assembly 36), ANL-6494 (January 1962).

20. W. G. Davey, P. I. Amundson, J. M. Gasidlo, and J. K. Long, ZPR-III Assembly 38, to be published as an ANL report.

21. J. C. Bates et al., ZPR-III Assembly 39, to be published as an ANL report.

APPENDIX I

REFERENCES FOR TABLE III

Assembly Number	Experimental Critical Mass	$\frac{(\Delta M/M)}{(\Delta k/k)}$	Heterogeneous Correction	Irregular Boundary Correction	Center-gap Correction	L/D
2A	14	14	14	14	14	14
5	14	a	14	14	14	14
6F	14	14	14	14	14	-
9A	14	14	14	14	14	-
10	14	14	14	14	14	1
11	14	14	a	14	14	14
12	14	14	14	14	14	14
14	14	14	14	14	14	14
16	14	14	14	14	14	14
17	14	14	a	14	14	14
20	1	c	a	a	a	1
23	17	d	a	a	a	17
24	17	e	a	a	a	17
25	g	g	a	a	a	g
29	17	2	a	a	a	17
30	3	3	3	a	a	3
31	18	18	18	a	a	18
32	17	b	a	a	a	17
33	17	b	a	a	a	17
34	17	4	4	a	a	17
35	f	f	f	a	a	f
36	19	19	19	a	a	19

[a] Estimated by the author using results on similar reactors.

[b] To be published as ANL reports.

[c] ZPR-III Memo 61.

[d] ZPR-III Memo 78.

[e] ZPR-III Memo 76.

[f] ZPR-III Memo 80.

[g] ZPR-III Memo 75.

APPENDIX II

REACTOR COMPOSITIONS

ZPR-III Assembly Number	Volume Percentage of Element in Core[a]											Reflector Type b
	U^{235} (18.75)	U^{238} (18.97)	Fe (7.85)	Ni (8.90)	Cr (6.91)	Al (2.70)	Na (0.84)	C (1.67)	O (2.55)	Mo (10.19)	Zr (6.44)	
2A	13.97	1.02	19.71	2.78	5.28	31.44						A
5	14.00	15.90	8.74	1.23	2.34	31.50						D
6F	14.00	15.90	8.81	1.24	2.36	31.40						A
9A	11.70	38.00	10.19	1.43	2.73	21.50						A
10	11.85	57.90	13.82	1.95	3.70							A
11	9.51	71.72	6.55	0.92	1.75							A
12	9.38	35.40	6.55	0.92	1.75			31.96				A
14	9.38	0.70	6.55	0.92	1.75			63.92				A
16	9.38	50.10	6.55	0.92	1.75			18.10				A
17	9.38	20.60	6.55	0.92	1.75			45.68				A
20	6.09	18.97	10.26	1.44	2.75	25.14				5.03	4.32	B
23	9.27	0.70	6.51	0.91	1.74	42.82						A
24	7.57	72.90	6.68	0.94	1.79							A
25	7.17	74.17	6.55	0.92	1.75							A
29	4.97	9.97	17.70	2.49	4.74	24.40			14.50			A
30	5.91	9.04	17.56	2.47	4.70	23.35			7.26			A
31	5.81	9.14	17.58	2.48	4.70	23.49						A
32	9.26	0.66	58.05	8.18	15.54							A
33	9.27	0.68	45.58	6.42	12.20		18.20					A
34	4.67	10.30	17.63	2.48	4.72	25.50		9.08				A
35	4.06	0.29	35.52	5.00	9.50		35.56		4.15			C
36	9.37	49.51	9.09	1.28	2.43		18.23					A

[a] At densities given in parentheses for each element (gm cm^{-3}).

[b] In all cases the reflector was 30.00 cm thick. There were four types with the following volume percentage compositions:

	U^{235}	U^{238}	Fe	Ni	Cr	Na	Al	Mo	
A	0.19	83.30	5.20	0.73	1.40				
B	0.10	45.39	13.92	1.96	3.72		10.08	2.46	
C	0.09	39.61	13.52	1.90	3.62	32.48		2.18	
D	0.08	39.70	5.24	0.74	1.40		24.60		Inner (18.1 cm thick)
	0.19	83.30	5.24	0.74	1.40		2.27		Outer (18.1 cm thick)

APPENDIX III

CENTRAL SPECTRA AND SPECTRAL INDICES

Assembly	2A	5	6F	9A	10	11	12	14	16	17	20
Group	Central Spectral Indices										
1	0.036	0.037	0.036	0.027	0.024	0.020	0.026	0.036	0.023	0.030	0.020
2	0.072	0.068	0.067	0.049	0.041	0.034	0.048	0.074	0.041	0.057	0.038
3	0.116	0.104	0.102	0.076	0.065	0.053	0.073	0.112	0.064	0.086	0.065
4	0.147	0.145	0.143	0.129	0.121	0.109	0.112	0.118	0.111	0.114	0.111
5	0.177	0.184	0.183	0.193	0.204	0.199	0.156	0.118	0.173	0.140	0.169
6	0.162	0.171	0.173	0.192	0.207	0.212	0.155	0.108	0.177	0.134	0.185
7	0.118	0.123	0.125	0.140	0.147	0.157	0.130	0.096	0.143	0.117	0.151
8	0.078	0.078	0.081	0.093	0.098	0.108	0.102	0.080	0.107	0.094	0.107
9	0.054	0.051	0.052	0.052	0.046	0.048	0.074	0.072	0.067	0.076	0.071
10	0.028	0.028	0.028	0.035	0.034	0.043	0.057	0.058	0.052	0.059	0.053
11	0.007	0.006	0.006	0.008	0.007	0.008	0.030	0.041	0.021	0.037	0.016
12	0.004	0.004	0.003	0.005	0.005	0.007	0.020	0.032	0.013	0.026	0.011
13	0.001	0.001	0.001	0.001	0.001	0.002	0.010	0.022	0.005	0.015	0.002
14							0.004	0.014	0.002	0.008	0.001
15							0.002	0.011	0.001	0.005	
16							0.001	0.008		0.002	
	Average Central Cross Sections (barns)										
$\sigma_f U^{235}$	1.387	1.384	1.385	1.402	1.399	1.420	1.537	1.701	1.480	1.596	1.462
$\sigma_f U^{233}$	2.171	2.172	2.175	2.214	2.219	2.253	2.379	2.553	2.317	2.444	2.296
$\sigma_f Pu^{239}$	1.791	1.785	1.784	1.773	1.765	1.763	1.815	1.909	1.788	1.846	1.779
$\sigma_f Pu^{240}$	0.7319	0.7123	0.7028	0.6107	0.5759	0.5202	0.5435	0.6324	0.5295	0.5711	0.5203
$\sigma_f U^{234}$	0.7137	0.6978	0.6892	0.6078	0.5795	0.5284	0.5376	0.6095	0.5293	0.5586	0.5206
$\sigma_f U^{236}$	0.2571	0.2446	0.2403	0.1898	0.1680	0.1433	0.1772	0.2415	0.1611	0.1995	0.1563
$\sigma_f U^{238}$	0.1172	0.1102	0.1081	0.0807	0.0692	0.0573	0.0778	0.1159	0.0680	0.0911	0.0649
$\sigma_c U^{238}$	0.1413	0.1418	0.1423	0.1520	0.1533	0.1607	0.1843	0.2135	0.1731	0.1948	0.1696
	Central Spectra										
$\sigma_f 3/\sigma_f 5$	1.565	1.569	1.570	1.579	1.587	1.587	1.548	1.501	1.566	1.532	1.571
$\sigma_f 9/\sigma_f 5$	1.291	1.290	1.288	1.264	1.262	1.242	1.181	1.122	1.208	1.156	1.217
$\sigma_f 0/\sigma_f 5$	0.528	0.514	0.508	0.436	0.412	0.366	0.354	0.372	0.358	0.358	0.356
$\sigma_f 4/\sigma_f 5$	0.514	0.504	0.498	0.433	0.414	0.372	0.350	0.358	0.358	0.350	0.356
$\sigma_f 6/\sigma_f 5$	0.185	0.177	0.174	0.135	0.120	0.101	0.115	0.142	0.109	0.125	0.107
$\sigma_f 8/\sigma_f 5$	0.0844	0.0796	0.0781	0.0575	0.0495	0.0404	0.0571	0.0681	0.0460	0.0571	0.0444
$\sigma_c 8/\sigma_f 5$	0.102	0.102	0.103	0.108	0.110	0.113	0.122	0.126	0.117	0.122	0.116

Assembly	23	24	25	29	30	31	32	33	34	35	36
Group	Central Spectral Indices										
1	0.036	0.017	0.016	0.019	0.021	0.022	0.019	0.021	0.018	0.015	0.023
2	0.072	0.029	0.028	0.039	0.044	0.044	0.041	0.046	0.038	0.033	0.040
3	0.112	0.046	0.044	0.066	0.076	0.077	0.080	0.088	0.067	0.065	0.063
4	0.144	0.099	0.097	0.100	0.114	0.123	0.125	0.128	0.107	0.096	0.115
5	0.162	0.193	0.191	0.141	0.160	0.174	0.195	0.186	0.148	0.143	0.193
6	0.156	0.214	0.214	0.146	0.162	0.179	0.187	0.186	0.155	0.167	0.206
7	0.120	0.163	0.164	0.140	0.141	0.139	0.137	0.135	0.132	0.146	0.151
8	0.080	0.116	0.118	0.108	0.102	0.096	0.092	0.092	0.102	0.113	0.104
9	0.062	0.052	0.054	0.087	0.076	0.068	0.062	0.061	0.082	0.084	0.050
10	0.038	0.050	0.052	0.072	0.057	0.049	0.037	0.034	0.069	0.059	0.038
11	0.011	0.010	0.011	0.033	0.022	0.015	0.011	0.011	0.033	0.027	0.009
12	0.006	0.009	0.009	0.028	0.017	0.011	0.009	0.008	0.028	0.026	0.006
13	0.001	0.002	0.002	0.011	0.005	0.002	0.003	0.002	0.011	0.011	0.002
14				0.005	0.002	0.001	0.001	0.001	0.005	0.006	
15				0.004	0.001		0.001	0.001	0.004	0.006	
16				0.001					0.001	0.003	
	Average Central Cross Sections (barns)										
$\sigma_f U^{235}$	1.411	1.438	1.443	1.591	1.497	1.450	1.431	1.424	1.582	1.595	1.414
$\sigma_f U^{233}$	2.200	2.281	2.288	2.455	2.333	2.274	2.255	2.242	2.445	2.465	2.240
$\sigma_f Pu^{239}$	1.796	1.763	1.763	1.825	1.797	1.784	1.780	1.782	1.824	1.827	1.767
$\sigma_f Pu^{240}$	0.7089	0.4784	0.4678	0.4776	0.5417	0.5711	0.5866	0.6076	0.4924	0.4602	0.5529
$\sigma_f U^{234}$	0.6894	0.4897	0.4796	0.4738	0.5366	0.5667	0.5852	0.6028	0.4883	0.4599	0.5567
$\sigma_f U^{236}$	0.2524	0.1260	0.1217	0.1514	0.1721	0.1782	0.1762	0.1899	0.1537	0.1396	0.1617
$\sigma_f U^{238}$	0.1154	0.0494	0.0473	0.0650	0.0738	0.0750	0.0728	0.0804	0.0644	0.0586	0.0671
$\sigma_c U^{238}$	0.1474	0.1667	0.1684	0.1998	0.1760	0.1647	0.1603	0.1570	0.1977	0.2012	0.1574
	Central Spectra										
$\sigma_f 3/\sigma_f 5$	1.559	1.586	1.586	1.543	1.559	1.569	1.576	1.574	1.545	1.545	1.584
$\sigma_f 9/\sigma_f 5$	1.273	1.226	1.222	1.147	1.201	1.231	1.244	1.251	1.153	1.145	1.250
$\sigma_f 0/\sigma_f 5$	0.502	0.333	0.324	0.300	0.362	0.394	0.410	0.427	0.311	0.288	0.391
$\sigma_f 4/\sigma_f 5$	0.489	0.341	0.332	0.298	0.359	0.391	0.409	0.423	0.309	0.288	0.394
$\sigma_f 6/\sigma_f 5$	0.179	0.0876	0.0844	0.0951	0.115	0.123	0.123	0.133	0.0971	0.0875	0.114
$\sigma_f 8/\sigma_f 5$	0.0818	0.0343	0.0328	0.0409	0.0493	0.0517	0.0509	0.0565	0.0407	0.0367	0.0475
$\sigma_c 8/\sigma_f 5$	0.105	0.116	0.117	0.126	0.118	0.114	0.112	0.110	0.125	0.126	0.111

APPENDIX IV

GROUP FISSION CROSS SECTIONS FOR U^{234} AND U^{236}

These were estimated from the Second Edition of BNL-325.

Group	σ_f U^{234} (barns)	σ_f U^{236} (barns)
1	1.55	0.90
2	1.50	0.94
3	1.50	0.74
4	1.15	0.46
5	0.90	0.02
6	0.25	
7	0.06	
8		
9		
10		
11		
12		
13		
14		
15		
16		